

A Completely Overlapped Ku- and Ka-band Dual-Polarized Phased Array for Simultaneous Terrestrial and Satellite Communications

Bumhyun Kim¹, and Wonbin Hong¹

¹ Pohang University of Science and Technology (POSTECH): dept. Electrical Engineering, Pohang, South Korea

* whong@postech.ac.kr

Abstract—This paper proposes an antenna designed with the shared aperture principle to operate in both the Ku and Ka bands and support dual polarization while the two antennas are completely overlapped on the same layer. Ku-band and Ka-band phased arrays are realized within the same volume without any increase in size. The inter-element spacing is optimized by using a shared aperture concept. The reflection coefficient features below -10 dB for each operating band. Additionally, both bands exhibit inter-port isolation exceeding 20 dB. Both simulated and measured results for the Ku band yield a beam steering angle greater than ± 40 degrees for both polarizations and a maximum gain of 10.3 dBi in a 1×3 array structure. For the Ka band, it is confirmed that a maximum beam steering angle is over ± 43 degrees for all polarizations, resulting in a peak gain of 13.1 dBi in a 1×5 phased array structure.

Index Terms—shared aperture, phased arrays, millimeter-wave, satellite communication, terrestrial communication, beam coverage.

I. INTRODUCTION

As the use of the millimeter-wave spectrum increases, it is becoming feasible to deploy expansive frequency resources to provide users with high data rates and ultra-low latency services such as automated navigation, mixed reality, radar, and satellite communication [1]. Furthermore, the upper-mid band, also known as the 6G frequency range 3 (FR3: 7-24 GHz) spectrum has recently received considerable interest as the accessible unlicensed spectrum [2]. Within this spectrum, the Non-Terrestrial Networks (NTN) or low earth orbit satellite communication has been focused and developed as the new applications [3]. It can provide mobile services from satellites to ground users as a solution to overcome Non-Line-of-Sight (NLOS) situations. Specifically, Ku-band (12-18 GHz) among 6G FR3 spectrum is utilized for the up and down link range of satellite communications [4].

Considering the emergence of new spectrums and applications, it is crucial to incorporate multiple antennas into a small form factor such as mobile devices while preserving their individual characteristics. From this point of view, there is a demand for multi- or dual-band antennas that are optimized for both real-estate and energy efficiency. Recent literatures [5]-[7] have covered studies about multi- or dual-band antennas. Despite numerous efforts detailed in other literature, the following challenges arise when attempting to

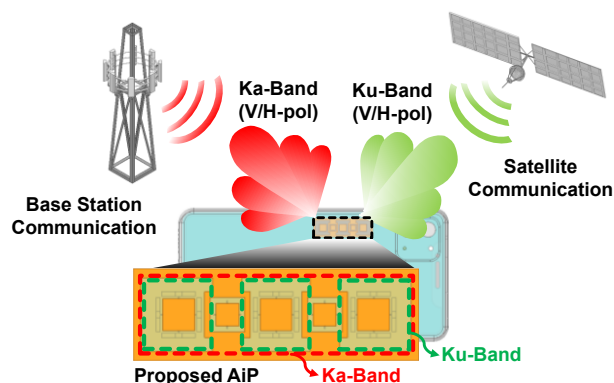
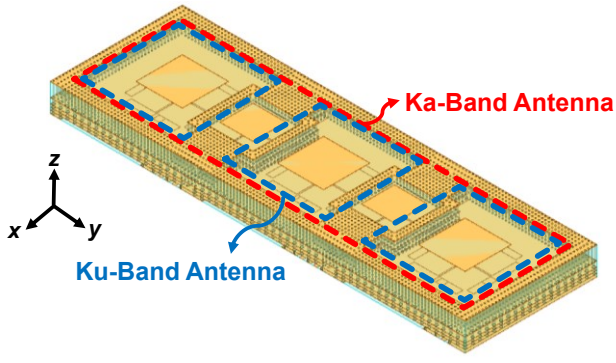


Fig. 1. The conceptual illustration of the proposed Ku- and Ka-band dual-polarized antenna-in-package within mobile devices for terrestrial and satellite communications.

apply it to mobile devices. First, separate antenna designs for different bands lead to larger antenna sizes [5]-[6]. Second, employing symmetric designs for dual polarization leads to the integration of the feed line more complex, especially hindering its extension into a linear array structure [5]-[6]. Third, it is challenging to keep the preferred beam steering angles consistent across all frequency bands when using extended array setups [7].

In response to the challenges previously mentioned, this paper introduces an antenna design based on the shared aperture principle, operating in both the Ku and Ka bands supporting dual polarization. The distinct features and innovations of the suggested Ku/Ka dual-polarized antenna include 1) utilizing the shared aperture technique results in a more simplified and compact antenna size, 2) dual-polarization architecture is formed into a linear one-dimensional array, making it especially compatible for integration into end-user devices, 3) adjusted inter-antenna spacing for both frequency bands allow for a wide beam scanning range. The proposed design can be potentially developed into an integrated antenna-in-package to support both satellite (Ku-band) and terrestrial (Ka-band) communications as illustrated in Fig. 1. Moreover, this multifunctional design can serve dual polarization in each band while maintaining high isolation. Section II discusses the proposed structure and operating principles. The fabricated

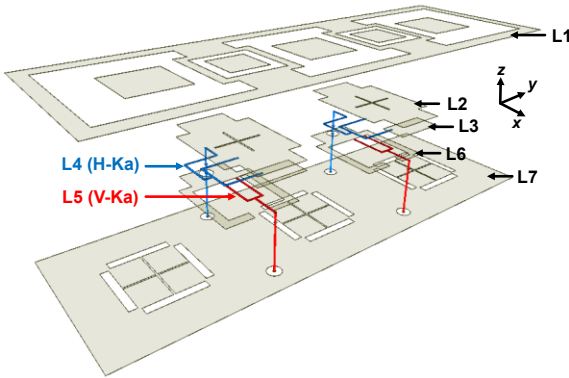


(a)

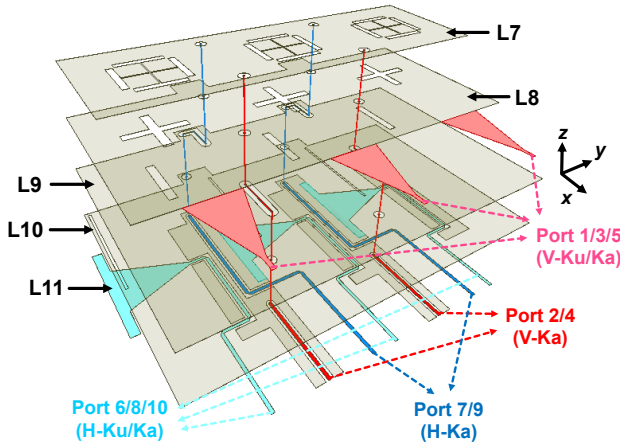


(b)

Fig. 2. Overall Structure of the proposed shared aperture Ku/Ka dual-polarized phased array antenna. (a) Isometric view. (b) yz -plane view.



(a)



(b)

Fig. 3. Exploded view of each layer of the proposed antenna. (a) Layer 1 to 7. (b) Layer 7 to 11.

proof-of-concept model and experimental results are presented in Section III. Section IV concludes this paper.

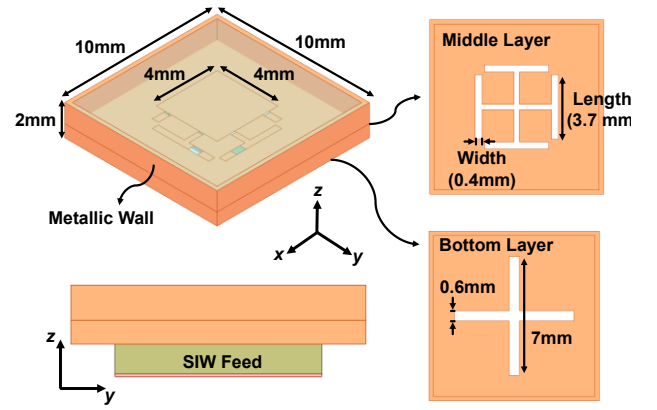


Fig. 4. The proposed Ku/Ka dual-polarized unit element.

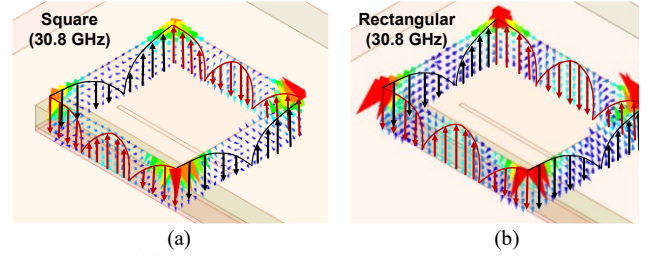


Fig. 5. E-field distribution of each radiator shape at TM 21 mode. (a) Square. (b) Rectangular

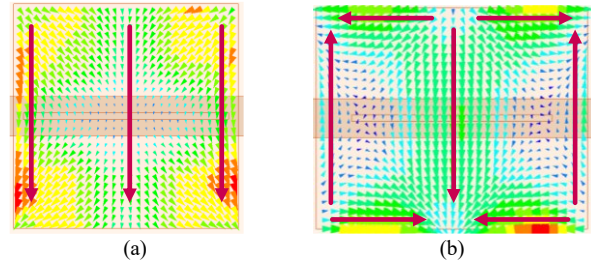


Fig. 6. J current distribution of each radiator shape at TM 21 mode. (a) Square. (b) Rectangular.

II. PROPOSED STRUCTURE AND OPERATING PRINCIPLES

A. Overall Structure and Stackup

The overall structure of the proposed shared aperture Ku/Ka dual-polarized antenna is presented in Fig. 2 (a). It is composed of 1×5 linear array structure ($31.4 \times 10 \times 2.11 \text{ mm}^3$), featuring five Ka-band antennas marked with red and three Ku-band antenna highlighted with blue. These elements are ingeniously positioned to share the common real-estate. A metallic via wall is integrated to clearly distinct between layers. The design is fabricated using the low temperature co-fired ceramic (LTCC) process ($\epsilon_r: 5.9, \tan\delta: 0.002$) due to the advantages of low loss tangent and facility to fabricate multi-layered design.

In terms of structure, it consists of 11 unique layers featuring $10 \mu\text{m}$ thickness. In Fig. 2 (b), layers 1 to 7 are allocated for the antenna, and layers 7 to 11 are designated for the antenna feeding networks and transition. Fig. 3 presents an exploded view of the proposed antenna stack up, including the feeding networks. It comprises a total of 10 ports to support

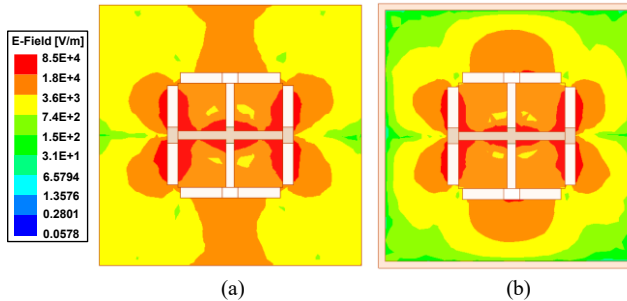


Fig. 7. E-field distribution at the middle layer at 28 GHz. (a) without metallic via wall. (b) with metallic via wall.

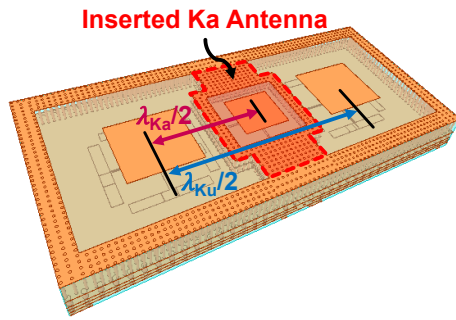
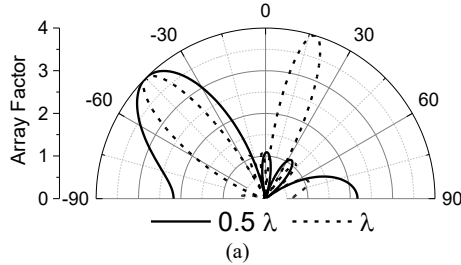


Fig. 8. (a) Array factor plots when four elements with different inter-spacing. (b) 1×3 phased array structure.

dual-band and dual-polarization functions. Regarding polarization, ports 1 to 5 are used for vertical polarization (x -axis) feeds, while ports 6 to 10 handle horizontal polarization (y -axis) feeds. With respect to frequency bands, ports 1,3, and 5, along with 6,8, and 10 are adaptable for both Ku and Ka bands. They use a substrate-integrated waveguide (SIW) for indirect coupling feed, which then transitions to a microstrip line structure. In contrast, ports 2,4,7, and 9 are specifically designed for the Ka-band, utilizing a strip line feed.

B. Proposed Ku/Ka Unit Element and Array Structure

The proposed structure for the Ku/Ka dual-polarization unit element is depicted in Fig. 4. It is designed as a square patch antenna with slot aperture coupling, surrounded by metallic via wall. The middle layer features symmetrically crossed I-shaped slots, facilitating the implementation of dual-polarization through an indirect feed structure. The signal is conveyed via the cross-slot in the bottom layer, utilizing the SIW structure. The antenna is designed to possess the dominant characteristics of the patch antenna in the 14.5 GHz Ku-band (TM 01 mode). In the 28 GHz Ka band, which is the second harmonic band, dual-band attributes are achieved. This is accomplished using the broadside TM 21 mode without

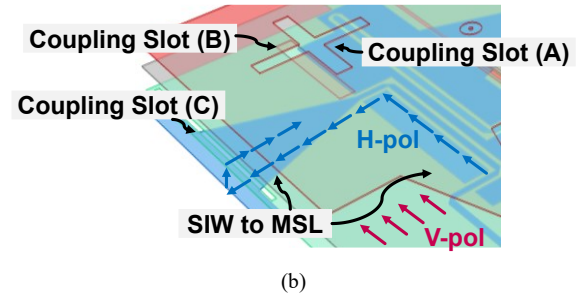
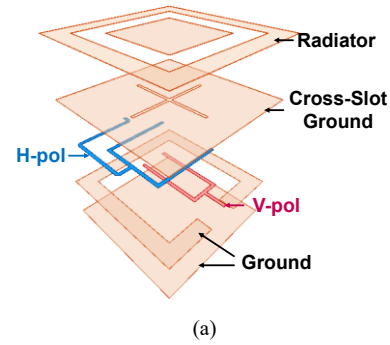


Fig. 9. (a) Exploded view of the Ka-band dual-polarized antenna. (b) Interconnection structure of the Ku/Ka-band dual-polarized antenna.

pattern distortion attributed to the slot feed, the square patch structure, and the encompassing metallic wall. To optimize impedance characteristics within second harmonic band, the width and length of the I-shaped slot in the middle layer are adjusted.

To better understand the broadside TM 21 mode in the second harmonic band, the E-field distribution is analyzed for a patch antenna with slot aperture feeding as shown in Fig. 5. Commonly, within slot aperture feeds, the second harmonic band facilitate TM 21 mode at both square and rectangular patch. This creates the E-field vectors at both edges to have opposite directions. However, a comparison of current distribution on the radiator surface as presented in Fig. 6 reveals that the square patch aligns all current vectors in-phase. This alignment allows for a broadside beam which is perpendicular to the radiator. In contrast, the rectangular patch shows current vectors along the length feature opposite directions at both edges and center, and a mirrored direction along the width from the center. This leads to mutual cancellation between current vectors, resulting in pattern divergence. Essentially, employing a square patch enables not only the realization of dual polarization through its symmetrical structure but also the broadside pattern achievement in the second harmonic band.

To explain the contribution of metallic wall in this structure, Fig. 7 shows the E-field distribution for both without and with metallic wall. Without the metallic wall in Fig. 7 (a), the ground plane at the middle layer features pattern distortion due to the effects of E-field surface waves. Conversely, when surrounded by the metallic wall in Fig. 7 (b), there is a significant decrease in the E-field magnitude from the surface wave, effectively confining the E-field within the metallic boundary. Due to the metallic wall acting as a

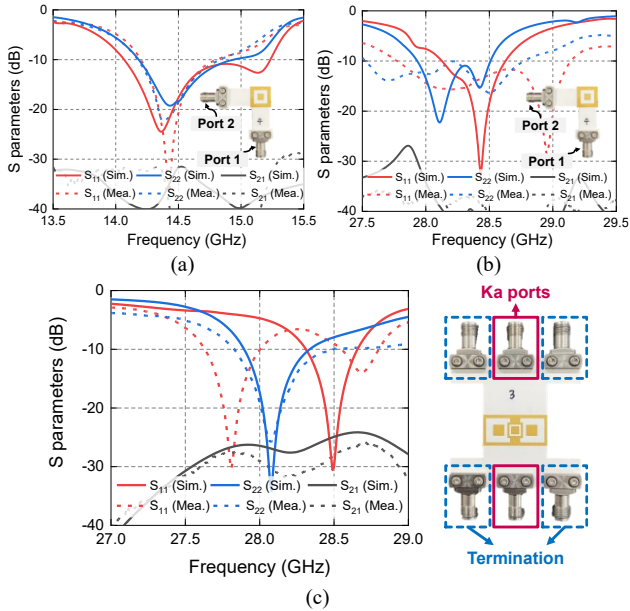


Fig. 10. Simulated and measured S parameters. (a) Ku-band of Ku/Ka antenna. (b) Ka-band of Ku/Ka antenna. (c) Central Ka-band antenna.

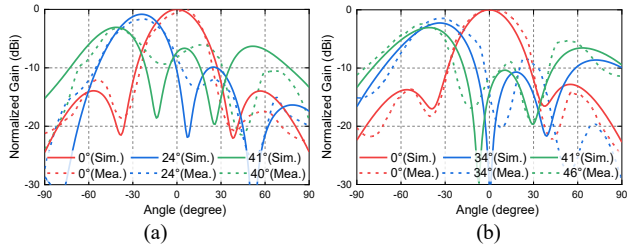


Fig. 11. Simulated and measured beam steering patterns at 14.5 GHz. (a) Vertical polarization. (b) Horizontal polarization.

clear boundary, it is possible to limit the interference from electromagnetic surface waves.

The fundamental concept applied in the extension of the proposed unit structure into an array design is described in Fig. 8. One of the prevalent challenges with conventional dual-band antennas is satisfying an optimal spacing that accommodates both bands. When configuring the proposed unit element at half-wavelength spacing in the Ku-band, it results in a wavelength spacing in the Ka-band. For instance, if we aim for a -45° beam steering using four antenna elements in Fig. 8 (a), it is confirmed that a beam formed at 0.5λ spacing exhibits a low side lobe. In contrast, a prominent grating lobe presents at 17° at λ spacing. Consequently, our innovative array design introduces a unique antenna structure, solely operational in the Ka-band, positioned between the existing Ku/Ka unit elements. This approach ensures optimal spacing for both frequency bands and facilitate wide beam steering capabilities. Essentially, by embedding this new antenna within the array, the shared aperture concept is utilized to enhance spatial efficiency without necessitating physical expansion of the primary array structure.

III. FABRICATED MODELS AND EXPERIMENTAL RESULTS

The central Ka-band antenna utilizes a feeding mechanism as depicted in Fig. 9 (a). To maintain polarization isolation,

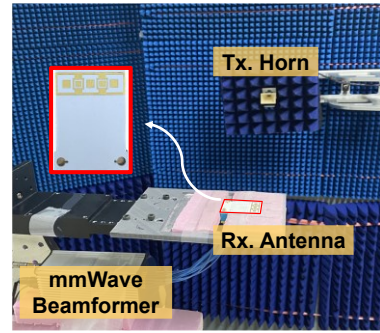


Fig. 12. Measurement environments of Ka-band radiation pattern.

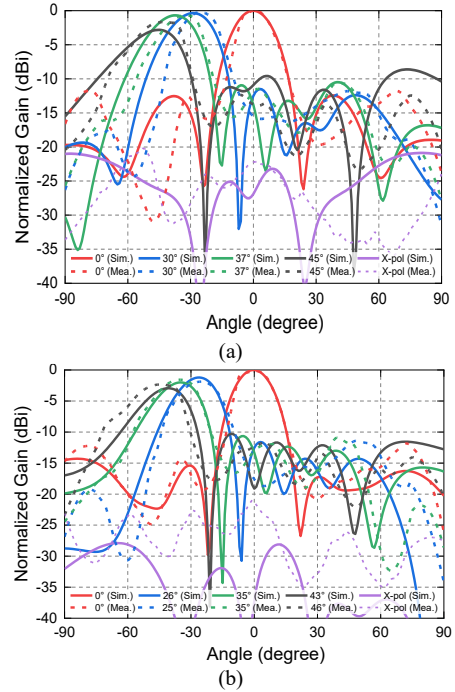


Fig. 13. Simulated and measured beam steering patterns at 28 GHz. (a) Vertical polarization. (b) Horizontal polarization.

indirect feeding methods are used. Additionally, a metallic wall boundary is contributed to reduce interaction with existing Ku/Ka unit elements. The signal is transmitted via a cross-slot ground located under the radiator, accompanied by two strip lines for each port on the below layer. Feed lines for vertical and horizontal polarizations are denoted by red and blue lines, respectively. Both feed lines utilize a U-shaped design to ensure a symmetrical radiation pattern. These feed lines are finally connected to the interconnection board through the vertical transition. In this paper, the detailed interconnection structure of these feeds is omitted.

Fig. 9 (b) illustrates the interconnection structure of the Ku/Ka antenna. Signals are relayed through a transition from the microstrip line to the SIW. The top crossed coupling slot facilitates the integration of two orthogonal feeds. The vertical polarization is achieved through an SIW between layers A and B, with signals passing through the coupling slot in layer A. For horizontal polarization, a SIW structure between layers B and C is employed. Signals transmit from the bottom layer to the coupling slot in layer C. They are then recoupled by the

TABLE I

Reference	[5]	[6]	This work
Frequency (GHz)	Ku/Ka (16/33.5)	Ku/Ka (16/34.7)	Ku/Ka (14.5/28)
Dimension (λ_0^3)	72.4 (4×4 Array)	5.37 (4×4 Array)	0.07 (1×5 Array)
Polarization	Dual LP (Ku) Dual CP (Ka)	Dual LP (V-Ku, H-Ka)	Dual LP
3dB Scan Angle	N.A.	$\pm 40^\circ$ (16) $\pm 40^\circ$ (34.7)	$\pm 43^\circ$ (14.5) $\pm 45^\circ$ (28.4)
Isolation (dB)	>15	>25	>30 (Ku) >20 (Ka)

slot in layer B, eventually reaching layer A. This flow is highlighted by the blue arrows.

The fabricated unit element and its S parameter results are presented in Fig. 10 (a) and (b). Within the Ku-band in Fig. 10 (a), the reflection coefficients for port 1 (v-pol) and port 2 (h-pol) are noted to be less than -10 dB in 14.21-14.8 GHz and 14.18-14.83 GHz, respectively, with maintaining isolation over 30 dB. In Ka-band results of Fig. 10 (b), the reflection coefficients for both ports are less than -10 dB within the 28.13-28.62 GHz and 27.94-28.5 GHz while staying over 30 dB of isolation. A 1×3 array design in Fig. 10 (c) is fabricated to validate the S parameters of a central antenna operated in the Ka band. This structure has six ports in total, with other ports except central ports are terminated. The measurement closely aligns with the simulation throughout 28 GHz band. Additionally, the mutual coupling coefficient between two ports is less than -20 dB across the operational bandwidth. The discrepancy between the simulation and measurement is mainly due to the tolerances in the fabrication process and the inevitable parasitic capacitance that occurs when connecting the signal line to the antenna.

The measured 1×3 phased array Ku-band beam steering patterns are presented in Fig. 11. Due to the lack of a phase-adjustable RFIC for the Ku-band, the beam steering capabilities are measured using passive power dividers and phase-shifted lines in the feeding networks. The maximum beam steering angles for both polarizations are over 40° in both simulated and measured results. The peak realized gains for both polarizations are higher than 10.1 dBi.

Fig. 12 shows the active phased array 1×5 antenna and measurement environment to verify the beam steering capability in the Ka-band. Within this frequency band, we utilize a 28 GHz mmWave 5G beamformer, equipped with 16 TRX RF channels. Each of these channels can individually adjust amplitude and phase. To connect the beamformer with the proposed 1×5 array antenna, the interconnection board is fabricated and assembled the entire system using 2×8 RF cable. In this test, 10 RF channels are used to analyze beam steering attributes in both vertical and horizontal polarizations. In Fig. 13, it is confirmed that the maximum beam steering angles are 45° and 43° for vertical and horizontal polarization, respectively. The maximum realized gains are 12.1 dBi for vertical and 13.1 dBi for horizontal polarizations. Table I presents the comparison of the proposed antenna with recent studies regarding dual-band antenna. Compared to [1] and [2] regarding Ku/Ka dual-band antenna, the proposed antenna can

be implemented with a smaller one-dimensional array structure that supports dual polarization. Additionally, it offers the advantages of achieving a wider beam steering angle independently in both frequency bands.

IV. CONCLUSION

This paper proposes a first-to-be-reported dual-polarized shared aperture antenna operated for both Ku and Ka bands for the first time. The two antenna arrays are completely overlapped resulting the smallest topology to be reported in literature. The antenna element utilizes slot aperture coupling, allowing for broadside radiation at both frequency ranges. By determining the ideal inter-element distance, it is extended to a phased array structure. This approach effectively resolves the typical challenge between array spacing and beam steering angles in dual-band systems, using the shared aperture concept. Our innovative 1×5 phased array antenna can support a beam coverage exceeding 82° in both the Ku and Ka bands for each polarization. Through the shared aperture consideration, the proposed antenna provides a space-efficient solution, addressing spatial constraints found in terminal devices. Considering its dual-band functionality, this design is expected to apply for revolutionizing satellite communications and millimeter-wave wireless technology.

ACKNOWLEDGMENT

This work was supported by Institute of Information & Communications Technology Planning & Evaluation (IITP) grant funded by the Korea government (MSIT) (No.2020-0-00858, 2023-00229817). The authors thank ANSYS Korea for their support.

REFERENCES

- [1] Y. Wang *et al.*, "A 39-GHz 64-Element Phased-Array Transceiver With Built-In Phase and Amplitude Calibrations for Large-Array 5G NR in 65-nm CMOS," *IEEE J. Solid-State Circuits*, vol. 55, no. 5, pp. 1249-1269, May 2020.
- [2] H. Kim, J. Kim and J. Oh, "Communication A Novel Systematic Design of High-Aperture-Efficiency 2D Beam-Scanning Liquid-Crystal Embedded Reflectarray Antenna for 6G FR3 and Radar Applications," *IEEE Trans. Antennas Propag.*, vol. 70, no. 11, pp. 11194-11198, Nov. 2022.
- [3] M. Giordani and M. Zorzi, "Non-Terrestrial Networks in the 6G Era: Challenges and Opportunities," *IEEE Netw.*, vol. 35, no. 2, pp. 244-251, Mar./Apr. 2021.
- [4] G. Gültepe, T. Kanar, S. Zehir and G. M. Rebeiz, "A 1024-Element Ku-Band SATCOM Phased-Array Transmitter With 45-dBW Single-Polarization EIRP," *IEEE Trans. Microw. Theory Techn.*, vol. 69, no. 9, pp. 4157-4168, Sep. 2021.
- [5] J. Ran, Y. Wu, C. Jin, P. Zhang and W. Wang, "Dual-Band Multipolarized Aperture-Shared Antenna Array for Ku-/Ka-Band Satellite Communication," *IEEE Trans. Antennas Propag.*, vol. 71, no. 5, pp. 3882-3893, May 2023.
- [6] Y. R. Ding and Y. J. Cheng, "Ku/Ka Dual-Band Dual-Polarized Shared-Aperture Beam-Scanning Antenna Array With High Isolation," *IEEE Trans. Antennas Propag.*, vol. 67, no. 4, pp. 2413-2422, Apr. 2019.
- [7] R. Lu, C. Yu, Y. Zhu, X. Xia and W. Hong, "Millimeter-Wave Dual-Band Dual-Polarized SIW Cavity-Fed Filtenna for 5G Applications," *IEEE Trans. Antennas Propag.*, vol. 70, no. 11, pp. 10104-10112, Nov. 2022.